RSC Advances

ROYAL SOCIETY OF CHEMISTRY

www.rsc.org/advances

Journal Name

ARTICLE

Synthesis and characterisation of 3-dimensional hydroxyapatite nanostructures using thermoplastic polyurethane nanofiber sacrificial template

Received 00th January 20xx,
Accepted 00th January 20xx

DOI: 10.1039/x0xx00000x

www.rsc.org/

R. Poorvisha[a], S. P. Suriyaraj[a], P. Thavamani[b], Ravi Naidu[b], Mallavarapu Megharaj[b], Amitava Bhattacharyya[c], R. Selvakumar[a,b*]

In this study, we report a facile synthesis of shape controlled three dimensional hydroxyapatite nanostructures (HAp) using sacrificial thermoplastic polyurethane (TPU) nanofiber template. TPU nanofiber synthesised using electrospinning process was used as template during the HAp synthesis through precipitation process. Various HAp morphologies including distinctly placed cylindrically porous HAp architecture, coral reef like, tightly packed fibrous sheet like and nanofiber like were synthesised using TPU nanofiber template. All the synthesised HAp were characterized using appropriate techniques like Fourier transform infrared spectroscopy (FTIR), X-ray diffraction (XRD), field emission scanning electron microscopy (FESEM) attached with selected area electron diffraction (SAED), energy dispersive X-ray spectroscopy (EDS) and X-ray photoelectron spectroscopy (XPS). The morphology, pore arrangement and the particle size of thenHAp varied significantly with varying dimensions of template and the template available per unit area of HAp. Hence, we have achieved four different 3D HAp morphologies using a single type of TPU nanofiber template. The TPU templated HAp nanostructures were more biodegradable than control HAp.

Introduction

Porous nanostructured materials are drawing attention of many researchers due to their smaller dimensions, high surface to volume ratio, tuneable pore size and the possibility of functionalization. Such materials have found immense applications in tissue engineering, drug delivery system, environmental remediation etc. Hydroxyapatites (HAp) have excellent biocompatibility, osteoconductivity, non-toxicity and flexibility[1]. They are synthesised using various methods like sol-gel, reverse microemulsion, hydrothermal, microwave-irradiation, solid-state reaction and precipitation process.[2] HAps have been used as bone fillers in orthopaedics and dentistry[3], as porous scaffolds in tissue engineering[4], as protein delivery agent[5] and in detection and adsorption of heavy metal ions from aqueous medium[6]. The performance of HAp can be increased by increasing the surface to volume ratio using porous soft and hard sacrificial templates. The soft template includes surface stabilizing molecules or polymers[7] and hard templates include porous solid materials such as anodic aluminum oxide (AAO)[8], ordered macroporous carbon (OMC)[9], mesoporous silica[10] etc. Various morphologies of HAp have been synthesised using the above mentioned types of templates. Cetyltrimethyl ammonium bromide was used as soft-template for synthesis of HAp nanorods.[7] Sea cucumber-like HAp was fabricated with the aid of Nafion N-117 cation exchange membrane[6] and hierarchical flower-like graphene oxide HAp was synthesized using biomimetic method[11]. Hard templating materials such as ordered macroporous carbon (OMC) template was used for making highly ordered porous HAp bioceramics.[9] CMK-3 (mesoporous carbon) and SBA-15 (mesoporous silica)[10] were used for the synthesis of mesoporous HAp nanostructures. Among these templates, polymer based templates are of particular interest due to their flexibility, ability to impart increased mechanical strength, biocompatibility and good processing/shaping properties.[12] Polymers can also act as nucleation sites for HAp and can influence the size and the orientation of the composite material[13]. They can act as template for HAp synthesis through dipole–dipole interactions, formation of covalent bonds and hydrogen bonds, or through complexation of Ca^{2+} ions with functional groups like amine, acetylamine, or hydroxyl etc.[14,15] Various types of polymers have been tried as templates for the synthesis of HAp based nanomaterials. Block copolymer synthesised using PMMA (poly-methyl methacrylate)[16] and poly(ethylene oxide)-b-poly(methacrylic acid) (PEO-b-PMAA) were used as template for the controlled synthesis of HAp nanoparticles in water[17]. Electrospunzein, a type of corn protein, was used as template to mineralise HAp.[18] However all these structures yield only one type of nanostructure and not much variation in nanostructure formation has been reported so far using single type of

[a] Nanobiotechnology Laboratory, PSG Institute of Advanced Studies,Coimbatore-641004, India
[b] Global Centre for Environmental Remediation (GCER), University of Newcastle, Callaghan, NSW-2308, Australia
[c] Advanced Textile and Polymer Research Laboratory, PSG Institute of Advanced Studies, Coimbatore 641004, India

† Footnotes relating to the title and/or authors should appear here.
Electronic Supplementary Information (ESI) available: [details of any supplementary information available should be included here]. See DOI: 10.1039/x0xx00000x

polymeric template. Among the polymers, thermoplastic polyurethane (TPU) is a phase segmented polymer having good hardness, mechanical and elastic properties. They are composed of soft and hard segments segregated as amorphous and pseudo-crystalline, respectively. The soft segments are made of long chains diols/polyol becoming the flexible segment and the hard segments are made up of combination of diisocyanate and short chain diols. The type of polyol used as soft segment determines its properties.[19] TPU is easy to process and possesses desirable properties such as elasticity, resistance to microorganisms, abrasion and excellent hydrolytic stability which makes them useful in many applications.[20]

Although TPU nanofibers have been used as a non-sacrificial templates for immobilisation of HAp[21,22] and other hybrid nanoparticles[23a,b], use of TPU nanofibers as single sacrificial template to obtain varying 3D morphology of HAp has not been reported so far. In the present study, we have used poly ether based electrospun TPU nanofibers as sacrificial template for the synthesis of various 3D HAp morphologies. The prepared HAp nanostructured materials were characterised using appropriate techniques and their phase purity, morphological properties and biodegradability have been studied.

Experimental

Materials

All chemicals used in this study were of analytical grade. Calcium nitrate tetrahydrate ($Ca(NO_3)_2{\cdot}4H_2O$) (purity > 99%), diammonium hydrogen phosphate ($(NH_4)_2HPO_4$) (purity > 99%), sodium nitrate ($NaNO_3$) (purity > 99%), sodium hydroxide (NaOH) (purity > 99 %), Tris-HCl buffer solution (purity ≥99 %), N, N-dimethyl formamide and acetone were procured from Merck, India. Texin 945 U grade thermoplastic polyurethane (TPU) was a gift from Bayer Material Science. All chemicals were used without further purification. Deionised water was used throughout the experiment.

Synthesis of TPU nanofiber template

TPU nanofiber template was prepared using electrospinning process according to Suriyaraj et al. [23a] The properties of the TPU pellets can be referred from Bayer Material Science LLC (Edition 2010-02-01). In brief, TPU solution was prepared by dissolving 1.0 g of TPU in N, N-Dimethylformamide and acetone in the ratio of 7:3 (v/v) followed by heating at 50 °C on a hot plate with vigorous stirring for 5h. The prepared polymeric solutions were electrospun (Electrospinning Unit, PSGIAS, India) onto grounded aluminium plate with the following experimental parameters; current supply of 30 kV, 18.5 cm working distance and 0.7 mL/h flow rate. The resultant TPU nanofiber was characterised using FESEM for morphology, bead formation and uniformity in fiber diameter and further used as template with varying dimensions.TPU membranes were finely cut manually into known dimensions ~1.0 mm^2, 0.5 cm^2, 1.0 cm^2 and 2.0 cm^2 sheets using a surgical scissor and used as template. In case of ~1.0 mm^2 nanofibers, nanofibers were cut mechanically using surgical scissors to smaller segments and then further size reduced using the laboratory blender.

Synthesis of control and TPU templated HAp

HAp was prepared by precipitation method.[24] In brief, 0.4 M solution of $(NH_4)_2HPO_4$, was added under constant stirring into 0.6 M solution of $Ca(NO_3)_2{\cdot}4H_2O$. The solution pH was maintained greater than 9 by addition of NaOH and the suspension was refluxed for 2 h. The white precipitate formed after 2 h of incubation was filtered, washed with copious amount of distilled water three times, dried overnight at 50 °C and calcined in air at 800 °C for 2 h. The resultant HAp was used as control (C-HAp). The templated HAp was synthesised using modified Eslami et al.[24] (**Fig. 1**). In brief, the synthesised TPU nanofiber membranes were taken in varying dimensions and added with 0.6 M solution of calcium nitrate followed by gentle stirring under room temperature for 6 h. 0.4 M $(NH_4)_2HPO_4$ solution was added dropwise to the $Ca(NO_3)_2{\cdot}4H_2O$/TPU mixture maintaining the Ca: P molar ratio at 1.67. In all cases, the ratio of Ca:P was maintained constant throughout the study. After a known incubation time, the precipitate obtained was filtered using 0.45µm Whatman filter and washed with copious amount of de-ionized water. The resulting precipitate was collected and dried at 50 °C overnight, followed by pyrolysis at 800 °C for 2 h.

Characterization

The resultant TPU templated HAp materials and C-HAp were analysed using different characterisation techniques. The morphology and elemental composition of the synthesised materials were analysed using field emission scanning electron microscopy (FESEM) (Sigma, Carl Zeiss, Germany) and energy dispersive X-ray spectroscopy (EDS) respectively. The crystal structure, lattice parameters and phases of C-HAp and template HAp were analyzed using X-ray diffractometer (XRD-600, Shimadzu, Japan) with generator settings of 30 mA, 40 kV; step size 0.001 (2 theta) with scan step time of 3.2 seconds in continuous mode. The surface functional groups were analysed using Fourier transform infrared spectroscopy (FTIR) (Nicolet Avathar-320 FTIR spectrometer, Madison) at a scan range of 400-4000 cm^{-1}. KBr was used along with milligrams of synthesized nanomaterial to make pellets and analysed at a scanning speed of 2 mm/sec at a resolution of 4 cm^{-1}. The chemical composition of the synthesised HAp was determined using an X-ray photoelectron spectroscopy (XPS) (SPECS SAGE) with a Phoibos 150 hemispherical analyzer and an MCD-9 detector at a take-off angle of 90°. A circular area of 3mm in diameter was used as scanning surface and Mg Kα (hν = 1253.6 eV) was used as X-ray source operated at 10 kV and 20 mA (200 W) with a background pressure of 1.5 x 10^{-5}mTorr. To obtain the spectra pass energy of 20 to 100 eV, energy steps of 0.1 to 0.5 eV were used. CASAXPS software (Neil Fairley, U.K.) was used to analyze the spectra. Degradability of synthesised material was investigated as per Singh (2012).[25] 0.2 g of HAp based material was taken and soaked in 50 mL of 0.05 M Tris-HCl buffer solution (pH 7.4) for 15 days. The samples were filtered and dried at 100 °C. The percentage weight loss of sample was calculated by the formulae (Eq. 1) given below:

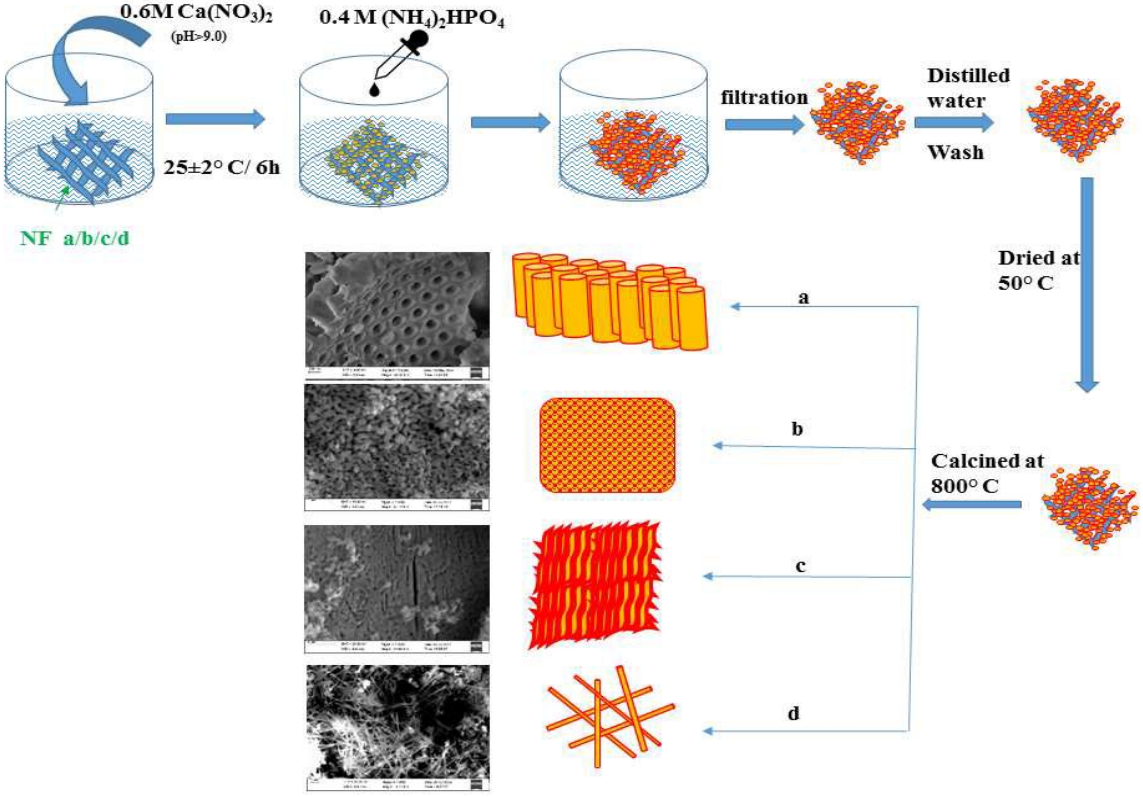

Fig. 1 Scheme representing the synthesis of various template HAp using TPU nanofibers (NF- nanofiber template; (a) ~1mm^2 (b) 0.5 cm^2 (c) 1.0 cm^2 (d) 2.0 cm^2 TPU template)

% weight loss= ((W1-W2)/W1)x100…… (1)

Where,W_1 is the initial weight of sample, W_2 is the final weight of sample after soaking inTris-HCl buffer solution.

3. Results and discussion

TPU nanofibers were synthesised using electrospinning process under optimised operating conditions. **Fig. 2** shows the FE-SEM image of the electrospun TPU nanofiber mat. The fibers were uniform and found to be without beads. The TPU nanofibers had an average fiber diameter of 350 ± 71 nm (**Fig. 2 inset**). Nanofiber mats that were finely chopped (~1.0 mm^2), and cut to known area (0.5 cm^2, 1.0 cm^2 and 2.0 cm^2) were used as template material.The C-HAp and TPU templated Haps were synthesised using calcium nitrate tetrahydrate and diammonium hydrogen phosphate via precipitation method. The reaction mechanism involved in the formation of the hydroxyapatite precipitate is as follows.[24]

$$10\ Ca(OH)_2 + 6(NH_4)\ 2HPO_4 \longrightarrow Ca_{10}(PO_4)6(OH)_2 + 6H_2O + 12\ NH_4OH \quad (2)$$

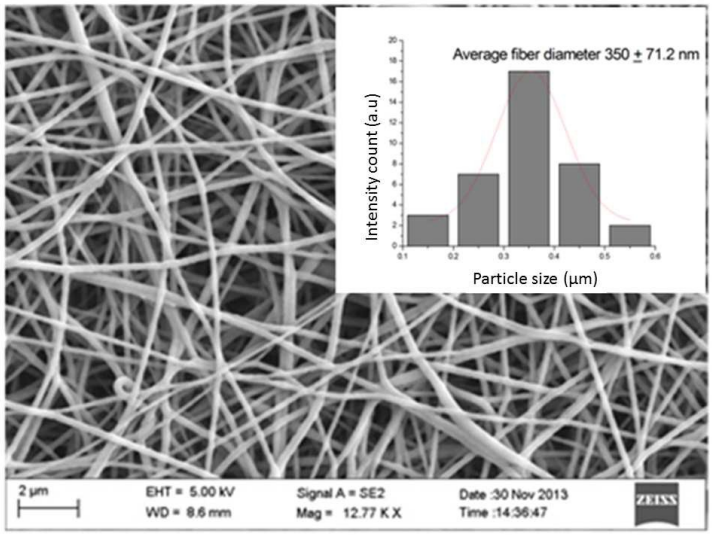

Fig. 2 FE-SEM image of TPU nanofiber membrane (inset: histogram showing fiber diameter)

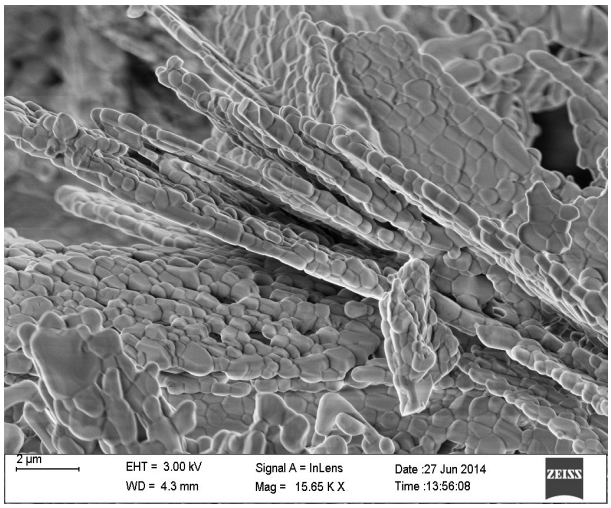

Fig. 3 FESEM image of C-HAp

The morphology, size and form of the HAp nanomaterial synthesised were determined using FE-SEM (**Fig. 3**). Figure 3 shows the SEM images of the C-HAp nanoparticles after pyrolysis. The C-HAp particles were found to be irregular, agglomerated and stacked one over the other with particle size ranging between 0.5 to 1.0 µm. Such agglomeration is due to pyrolysis which ultimately leads to decrease in surface area and porosity through particle coalescence and increase in density.[26] When nanofibers were introduced as template at the beginning of the HAp precipitation protocol, sequential accumulation of cations (calcium) and anions (phosphate) resulting in HAp synthesis onto and in between the surface was expected. On further pyrolysis of the HAp-TPU nanofibers mixture, the pyrolysis process induces complete weight loss and degradation of the TPU at 800 °C resulting in formation of pores. The literature on thermal stability of the TPU was used as an index for temperature selection to achieve near 100% weight loss/thermal degradation of TPU present in between the formed HAp. The temperature for template removal was kept double the final degradation temperature (T_{end}-400.4 °C)).[27] Bajsic *et al*.[27] reported 0.7% residual TPU at T_{end} of 700 °C using thermo gravimetric analysis. Hence it is evident that the residual TPU present in the HAp-TPU nanofiber mixture will be very less after pyrolysis at 800 °C. A uniform removal of TPU from the HAp-TPU nanofiber mixture without much variation in the HAp morphology was expected at increasing dosage of TPU nanofibers. However the morphology of the HAp nanoparticles varied largely with respect to the template dosage and the structure used during the HAp synthesis **(Fig. 4)**.

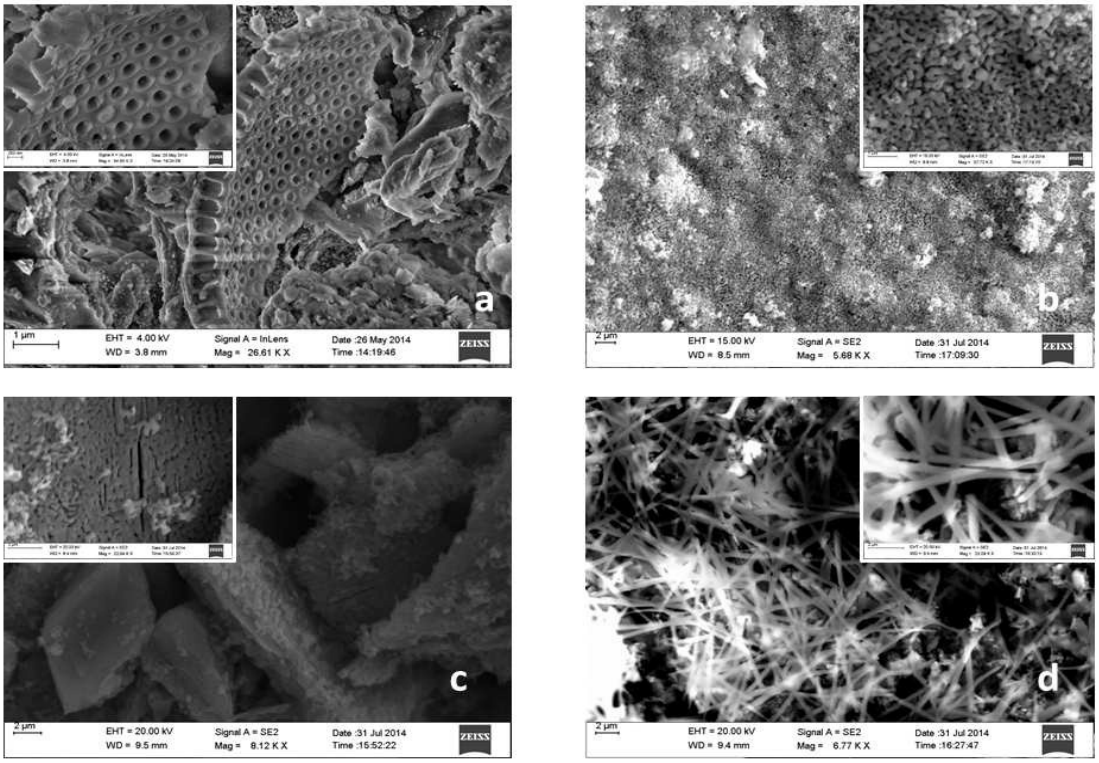

Fig. 4 FESEM image of various TPU templated HAp (a) ~1mm^2 TPU template, (b) 0.5 cm^2 TPU template, (c) 1.0 cm^2 TPU template, (d) 2.0 cm^2 TPU template (Insets: High magnification image

Journal Name

ARTICLE

When finely chopped nanofiber (~1.0 mm^2) was used as template, two different HAp morphologies were obtained. Few particles were irregular, porous, agglomerated and submicron in size. Along with agglomerates, a highly ordered, nanoporous architecture of HAp was found with uniform size and dimensions (**Fig. 4a**). The pores were found to be placed at regular intervals in that porous structure with average external diameter of 248±34 nm and internal diameter of 178±18 nm. The pores were found to extend like regular channels with an average length of 534±46 nm (**Fig. 4a and inset**). When varying length of nanofiber sheets were introduced as template, the morphology of HAp was totally different. With 0.5 cm^2 nanofiber template, porous, coral reef like HAp morphology was formed **(Fig. 4b)**. The pores were clearly distinct and were irregular in nature when visualised at higher magnification (**Fig. 4b inset**). The particles were found to be fused with each other to form a network that looks similar to a sieve. When the sheet size was extended to 1.0 cm^2, the HAp appeared like flakes **(Fig. 4c)**. The HAp took the morphology of the nanofiber after pyrolysis and was closely packed (**Fig. 4c inset and Supplementary Fig. S1**). The number of pores were found to be very few when compared to other materials synthesised during the study. As the size of the nanofiber sheet was further extended to 2.0 cm^2, the HAp morphology resembled of a typical nanofiber morphology (**Fig. 4d**). The average diameter of the individual fiber shaped HAp particle was 0.25 ± 0.02 µm (**Fig. 4 d inset**). The elemental composition confirmed the presence of Ca, P, C and O in the synthesised nanoporous HAp when studied using EDS (**Supplementary Fig. S2)**. The presence of carbon in the matrix might be contributed by the sacrificial TPU nanofibers template. XRD analysis was used to confirm the crystalline phase formation, degree of crystallinity and crystallite size of the synthesized HAp materials **(Fig. 5)**.

The X-ray diffraction profiles of C-HAp nanoparticles showed hexagonal crystal structure with unit cell parameters of a= 9.424 Å, b= 6.879 Å and space group $P6_3/m$ (176) and were in correlation with JCPDS data base (card no: 74-0566).[28] The crystalline peaks at 2θ = 28.92^0 (211), 30.95^0 (211), 32.20^0 (112), 34.20^0 (202), 38.70^0 (220), 40.09^0 (221), 44.75^0 (400), 49.26^0 (213), 52.30^0 (303) and 56.7^0 (500) and the corresponding 'hkl' valves, confirmed the formation of hydroxyapatite structure. The C-HAp nanoparticles were highly crystalline as a result of pyrolysis.[29] There were slight shifts in the peaks observed when the TPU was incorporated into the HAp indicating possible modification in the HAp structure. However, all the templated

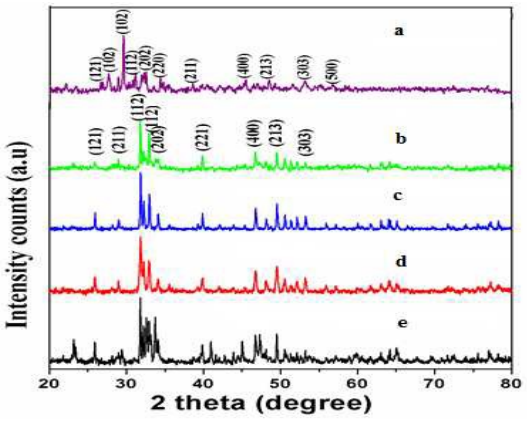

Fig. 5 XRD spectra of various TPU templated HAp ((a) C-HAp, (b) ~1mm^2 TPU template, (c) 0.5 cm^2 TPU template, (d) 1.0 cm^2 TPU template, (e) 2.0 cm^2 TPU template).

HAps also had hexagonal crystal structure having cell parameters a= 9.424 Å, b= 6.879 Å and space group $P6_3/m$ (176) as reported in the JCPDS data (card no: 74-0566).[28] The crystalline peaks and the corresponding 'hkl' values of HAp found in the TPU template HAp confirmed the formation of HAp structure. Along with the HAp crystalline peaks, few additional peaks were found in the TPU template HAp. The templated materials were all crystalline and phase pure due to high pyrolysis temperature. The surface functional groups present in TPU nanofibers, C-HAp and the TPU templated HAp were analysed using FTIR spectroscopy (**Fig. 6**). The TPU nanofibers showed peaks at 1072 cm^{-1}, 1699 cm^{-1}, 2861 cm^{-1} and 2942 cm^{-1} indicating the presence of C-O-C stretching, C=O urethane, asymmetric and symmetric stretching of CH_2 group respectively (**Fig. 6 a**).[30,23a] The FTIR spectra of the C-HAp **(Fig. 6 b)** had a band at 3495 cm^{-1} indicating stretching vibrations of hydroxyl group. The band at 563.21 cm^{-1} belonged to the bending vibration of the –OH and 1026.13 cm^{-1} and 910.40 cm^{-1} bands are characteristics of the phosphate stretching vibration. The bands corresponding to the phosphate bending vibrations[31] were observed at 732.95 cm^{-1} and 524.46 cm^{-1}, whereas the doublet at 563 and 524 cm^{-1} corresponds to the O-P-O bending mode. The peak at 1381.03 cm^{-1} corresponds to the carbonate group in the HAp structure. TPU templated HAp synthesized using varying dimensions of nanofibers had the IR pattern similar to control Hap **(Fig. 6c-f)**.

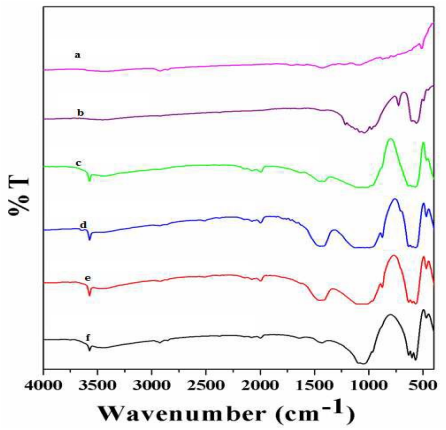

Fig. 6 FTIR spectra of control and TPU templated Hap ((a) TPU nanofiber, (b) C-HAp, (c) ~1mm^2 TPU template, (d) 0.5 cm^2 TPU template, (e) 1.0 cm^2 TPU template, (f) 2.0 cm^2 TPU template).

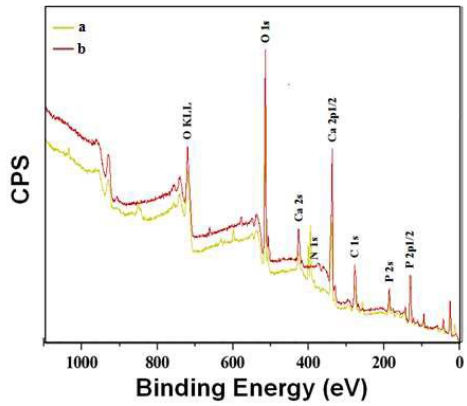

Fig. 7 XPS spectra of control and TPU templated HAp ((a) C-HAp, (b) 2.0 cm^2 TPU template).

The TPU templated HAp had a new peak, formed at 3572.17 cm^{-1} corresponding to the –OH bands.[32] The peak position at 1435.03 cm^{-1} corresponding to CO_3^{2-} group appeared to be intense in TPU template HAp. Peak broadening was observed in the regions between 1103.28 and 1018.41 cm^{-1} which is the characteristic band for the phosphate stretching vibration. The band at 632.65 cm^{-1}, 601.79 cm^{-1} and 570.93 cm^{-1} corresponds to the P-O bending mode.[33] Thus the change in the intensity of the peaks and the peak broadening were observed in case of the nanoporous HAp synthesized through TPU templating. XPS analysis was carried out to analyze the surface composition of selected representative materials (C-HAp and 2.0 cm^2 TPU template HAp) **(Fig. 7)** based on the FTIR and XRD pattern. The general XPS scan revealed the presence of pure HAp without any traces of metallic and other impurities. The major peaks, found in the XPS spectra, were in good agreement with the reported literature[34,35] and were attributed to the chemical state of Ca, P and O elements in the HAp matrix.[36] The photoelectron lines of control HAp **(Fig. 7a)** has a binding energy of about 285, 534, 346, 437, 134 and 190 eV attributed to C 1s, O 1s, Ca 2p, Ca 2s, P 2p $_{1/2}$ and P 2s, respectively. The elemental ratio of Ca/P in HAp was 1.63, which is in reasonable agreement with the standard value of HAp (1.67). The XPS narrow scan reveals one peak, located at binding energy of 346 eV and 350 eV attributed to Ca 2p3/2 and Ca 2p1/2, respectively. The O1s peak near 532 eV is due to oxygen associated with phosphate group in HAp and adsorbed water. The spectrum includes peaks labelled O KLL at 752 eV, and represents the energy of the electrons ejected from the atoms due to the filling of the O 1s state (K shell) by an electron from the L shell coupled with the ejection of an electron from an L shell.[37] For the polymeric templated HAp nanoparticle, the peak positions and the binding energy of the Ca, P and O were similar to the calcined native HAp sample. The polymeric templated samples had carbon peaks, with a binding energy of 284 eV attributed to C 1s. Carbonate-type carbon were observed in the C (1s) region for all the samples **(Fig. 7b)**. Quantifying the elements observed in the survey scans, Ca/P ratio has been determined by taking the area under the characteristic peaks of Ca 2p and P 2p. The synthesised HAp materials exhibited Ca/P elemental ratio of 1.63. C-HAp and 2.0 cm^2 TPU templated HAp samples were subjected to degradation studies using 0.05M tris-HCl at 7.4 pH. The study showed that there was no statistically significant weight change observed after 3 days of exposure. However the materials started degrading as the incubation time was extended. The C-HAp possessed 3.93 ± 0.2 % degradation after an exposure time of 15 days. Pyrolysis was found to greatly inhibit the degradability of the HAp. The weight loss was further attributed to the loss of calcium ion, which resulted in an increase in pH of the buffer medium from 7.4 to to 8.32. 2.0 cm^2 TPU templated HAp samples showed increased degradation rate (4.14 ± 0.9 %) when compared to C-HAp after 15 days of incubation. Singh (2012)[25] has reported 5 % degradability with calcined HAp after an exposure time of 15 days to tris-HCL buffer. The increased degradation rate with templated HAp may be attributed to the porosity. Increased porosity results in an increase in the surface area of the material, thereby providing more space for the biodegradation of the material by increasing the interaction between the TPU templated HAp and the aqueous medium[38]. Thus the degradation occurs more quickly in porous than non-porous HAp materials.

Mechanism of change in HAp morphology

When the precipitation of hydroxyapatite occurs on the surface of the TPU nanofibers, a strong gel like mass was formed through the electrostatic interaction of the calcium phosphate with nanofibers. Such gels lead to the formation of organised structures, keeping the nanofibers intact within the HAp gel system. When they get solidified, the structure of the nanofiber added is immobilised within the formed HAp matrix. During pyrolysis process, the template decomposes into gases, such as CO_2 and HO, and leads to formation of pores.[39] Since the melting temperature of TPU is high (195-205 °C), gradual increase in pyrolysis temperatures allows gradual decomposition and diffusion of the polymeric material into the

HAp matrix without any pressure build-up.[40] However the rate of decomposition is dependent on the concentration of the TPU immobilised between a unit area of HAp matrix which ultimately decides the extent of diffusion into the HAp in that unit area. The elastomeric property of the TPU during heating and cooling also contributes to the template structures of HAp matrix. The hard domains in TPU can act as physical crosslinker, playing a role similar to chemical crosslinks, imparting elastomeric behavior to material. These hard domains can also occupy significant volume of material as effective nano-scale fillers before degradation at elevated temperature[41].

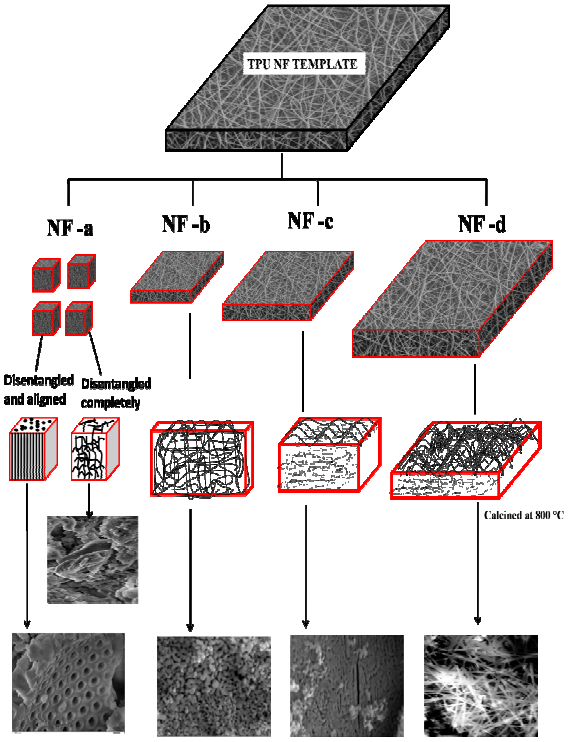

Fig. 8 Possible mechanism of synthesis of various morphologies of HAp using TPU nanofibers as template (NF- nanofiber; (a) ~1mm^2 TPU template, (b) 0.5 cm^2 TPU template, (c) 1.0 cm^2 TPU template, (d) 2.0 cm^2 TPU template)

In the present study, the amount and orientation of immobilised nanofibers within a unit area of HAp could possibly control the change in morphology of the HAp formed after pyrolysis as described in the scheme **(Fig. 8).** In the first set of experiment, ~1mm^2 chopped TPU nanofibers were used as template for HAp deposition on surface followed by precipitation and pyrolysis. During the mixing process, finely chopped TPU nanofibers get disentangled due to the lower entanglement density because of smaller size of TPU nanofiber mat and few become aligned to each other in the HAp matrix, followed by gradual evaporation of template leaving a defined regular TPU fiber morphology behind (**Fig. 4a inset**). However, in the places where this aligned nanofibrous templates are not available and where the other disentangled nanofibers arranged at random, they form irregular, porous, submicron sized HAp nanoparticles (**Fig. 4a**). During the mixing process, the nanofibrous mats would try to lay in two dimensions which would be strongly influenced by the size of nanofibrous mats. With the increase in size, they will gradually shift to two dimensional laying arrangements from complete 3D distribution i.e. the big nanofibrous mats will try to settle at the bottom of the mixing plate giving the complete impression of the nanofibrous mat upon pyrolysis as in case of Figure 4 d. Figures 4 b and c are the intermediate steps between these two extremities i.e. partially arranged towards 2D with increase in chopped mat size.

During subsequent set of processing, the orientation of the nanofiber remain fixed and the amount of nanofiber per unit area of HAp was increased by adding 0.5 cm^2 TPU nanofibers. Due to such an arrangement, the unit area available for HAp matrix formation within the TPU template is reduced to an extent, ultimately leading to more availability of template. As the template area was further increased to 1.0 cm^2 and 2.0 cm^2, the availability of nanofiber was more than the available HAp matrix in a unit area resulting in the reversal of diffusion. During the pyrolysis process, higher concentration of template acts like a binder of HAp with the nanofiber morphology in the available orientation. On subsequent cooling of the mixture, the 1.0 cm^2 and 2.0 cm^2 template HAp mixtures yield fibrous tightly packed sheet like and typical nanofiber like morphologies respectively (**Fig. 4c and d insets**). Since the HAp morphology with respect to addition of increased template area is leading to the formation of fiber like morphology, further increase in nanofiber size beyond 2.0 cm^2 is expected to result in similar type of HAp with distinct fiber morphology. However, further experiments are needed to confirm the possibility. The diffusion of the TPU polymeric template into the matrix leads to a small change in the surface functional group (**Fig. 6**) and the crystal structure of HAp (**Figure 5**) while maintaining the Ca:P ratio of 1:63 (**Fig. 5 and Supplementary Fig. S2**). The polymer and HAp interaction can also be correlated with respect to the formation of possible intermolecular bonds, polymer crosslinking during the calcination process and polymer percolation during the structure formation.[42,43] Hence with a single type of TPU nanofibrous template, we have shown that four different morphologies of HAp can be achieved.

Conclusion

The control and TPU templated HAp nanoparticles were synthesized using wet chemical precipitation method. TPU nanofibers prepared by electrospinning process having a diameter of 350 nm ± 71nm was used as template. Nanofibrous mats of dimensions of ~1.0 mm^2, 0.5 cm^2, 1.0 cm^2 and 2.0 cm^{2}were used as templating material with same reaction conditions. The templated TPU-HAp precipitates were pyrolysed at 800°C and cooled to room temperature. The resultant HAp materials were characterised using appropriate techniques. The FESEM characterization confirmed the morphological variations in the templated nanostructures. Various 3D structures such as distinctly placed cylindrically porous, coral reef like, tightly packed fibrous sheet like and

nanofiber like HAp morphologies were achieved. The characterization studies like XRD, FTIR and XPS confirmed the elemental composition, crystallinity and phase purity of the HAp nanostructures. The TPU templated HAp nanostructures were comparatively more biodegradable than control HAp.

Acknowledgements

The authors are thankful to Water Technology Initiatives (WTI), Department of Science and Technology, Government of India for funding this study (Sanction no: DST/TM/WTI/2K13/137). Support and help rendered by PSG Management and PSG Institute of Advanced Studies is acknowledged. COE medical textiles, South India textile research association (SITRA) is acknowledged for helping us through FE-SEM imaging. The authors are thankful to Bayer Material Science for providing polymers.

References

1 E. C. S. Rigo, A. O. Boschi, M. Yoshimoto, S. Allegrini Jr., B. Konig Jr. and M. J. Corbani, *Mater. Sci. Eng.*, C, 2004, **24**, 647-651
2 M. P. Ferraz, F. J. Monteiro and C. M. Manuel, *J. Appl. Biomater. Biom.*, 2004, **2**, 74-80.
3 S.V. Dorozhkin and M. Epple, *Angew. Chem. Int. Ed*., 2002, **41**, 3130-3146.
4 S. J. Hollister, *Nat. Mater*., 2005, **4**, 518-524.
5 W. Paul and C. P. Sharma, *J. Mater Sci*., 1999, **10**, 383-388.
6 Y. Zhang, Y. Liu, X. Ji, C. E. Banks and W. Zhang, *Chem. Commun.,* 2011, **47**, 4126-4128.
7 N. K. Nguyen, M. Leoni, D. Maniglio and M. Claudio, *J. Biomater. Appl.*, 2012, 1-13.
8 Y. Zhang, Z. Liheng , L. Li, X. Naicun, X. Xiudong and L. Jinghong, *Chem. Phys Lett*., 2003, **376**, 493-497.
9 L. Ji, J. Gavin, D. Yixiang, J. R. Jones and M. M. Stevens, *Chem. Commun*., 2011, **47**, 9048-9050.
10 Z. Xia, L. Libing and Z. Senlin, *Mater. Res. Bull*., 2009, **44**, 1626-1629.
11 T. Wen, W. Xilin, L. Mancheng, X. Zhouhao, W. Xiangke and X. An-Wu, *Dalton Trans*., 2014, **43**, 7464-7472.
12 M. Neumann and M. Epple, *Eur. J. Trauma*, 2006, **2**, 125-131.
13 S. Schachschal, P. Andrij and A. J. Hans, *Colloid. Polym. Sci*., 2007, **285**, 1175-1180.
14 Z. Li, L. Yubao, Y. Aiping, P. Xuelin, W. Xuejiang and Z. Xiang, *J. Mater. Sci- Mater. Med*., 2007, **16**, 213-219.
15 V. M. Rusu, C. H. Ng, M. Wilke, B. Tiersch, P. Fratzl and M. G. Peter, *J. Biomater*., 2005, **26**, 5414-5426.
16 W. Tjandra, P. Ravi, J. Y. Kam and C. Tam, *Nanotechnology,* 2006, **17,** 5988-5994.
17 J. H. Lee, I. T. Kim, R. T. Meisha and L. Shofner, *J. Mater. Chem.,* 2012, **22**, 11556-11560.
18 C. Yao, L. Yueling and F. W. Zein, *Polym. Composite.*, 2013, **34**, 1163-1171.
19 G. R. E. Maries and V. Manoviciu, I, Analele Universităţii din Oradea, Fascicula Arte Vizuale, Editura Universităţii din Oradea, Oradea, 2005, **2**, 125-133.
20 A. Pedicini and R. J. Farris, *J. Polym.*, 2003, **44**, 6857-6862.
21 F. A. Sheikh, M. A. Kanjwal, J. Macossay, N. A. M. Barakat and H. Y. Kim. *Express Polym. Lett*., 2012, **6**, 41-53.
22 H. Y. Mi, S. M. Palumbo, X. Jing, L. S. Turng, W. J. Li and X. F. Peng. *J. Biomed. Mater. Res.,* 2014, **102B**, 1434-1444.
23 a) S. P. Suriyaraj, B. Amitava and R. Selvakumar, *RSC Adv*., 2015a, **5**, 26905-26912.
b) S. P. Suriyaraj, M. P. Mamatha, B. Amitava and R. Selvakumar, *RSC Adv*., 2015b, **5,** 68420.
24 H. Eslami, M. Solati-Hashjin, M. Tahriri and F. Bakhsh, *Mater. Sci-Poland*, 2010, **28**, 5-13.
25 A. Singh, *Bull. Mater. Sci.*, 2012, **35**, 1031-1038.
26 S. Bailliez and A. Nzihou, *Chem. Eng. J*., 2004, **98**, 141-152.
27 E. G. Bajsic, R. Vesna and S. Ivana, *J. Polym*., 2014, Article ID 289283, 1-8.
28 International Centre for Diffraction Data, JCPDS card No. 74-0566
29 S. B. Erzsébet, B. Réka , S. Alexandra, D. Valentina and I. Baldea, *Chem. Pap. - Chem. Zvesti*, 2009, **63**, 568-573.
30 J. H. S. A. Júnior, D. A. Bertuol, A. Meneguzzi, C. A. Ferreira and F. D. R. Amado, *Mat. Res*., 2013, **16**, 860-866.
31 F. Chen and Z. Wang, *Mater. Lett*., 2002, **57**, 858-861.
32 S. Gao, R. Sun, Z. Wei, H. Zhao, H. Li and F. Hu, J. Fluorine Chem., 2009, **130**, 550-556
33 C. Liang, M. M. Joseph, C. M. J. Lee and H. Li, *Nanotechnology*, 2011, **22,** 105708.
34 G.N Raikar, J.L Ong, L.C. Surf Sci Spec., 1997, 4, 9–12.
35 Y. Yoshida, Nakayama Y, Snauwaert J, Hellemans L, Lambrechts P, Vanherle G and Wakasa K, J. Dental Res. 2000, **79,** 709-714
36 M. P. Mahabole, R. C. Aiyer, C. V. Ramakrishna, B. Sreedhar and R. S. Khairnar, *Bull. Mater. Sci*., 2005, **28**, 535-545
37 H.B. Lu, C.T. Campbell, D. J. Graham, and B. D. Ratner, Analy. Chem., 2000, **72**, 2886-2894
38 J. S. Temenoff and A. G. Mikos, Chapter 5: Biomaterial degradation, Pearson Prentice Hall, Upper Saddle River, New Jersey, 2008, 178.
39 E. Salimi, J. Javadpour and M. Anbia, *ISRN Ceramics*, 2012, **2012,** Id: ID 960915, 6 pages
40 J. Saggio-Woyansky, C. E. Scott and W. P. Minnear, *Am. Ceram. Soc. Bull*., 1992, **71**, 1674-1682.
41 Z. Petrovic, J. Ferguson, Prog. Polym. Sci., 1991, **16**, 695-836.
42 L.A. Cyster, D. M. Grant, S. M. Howdle, F.R.A.J. Rose, D. J. Irvine, D. Freeman, C.A. Scotchford, K. M. Shakesheff, Biomaterials, 2005, **26**, 697-702.
43 N. Tamai, A. Myoui, T. Tomita, T.J. Nakase, T. Ochii, H. Yoshikawa, J. Biomed. Mater. Res, 2002, **59,** 110-117.

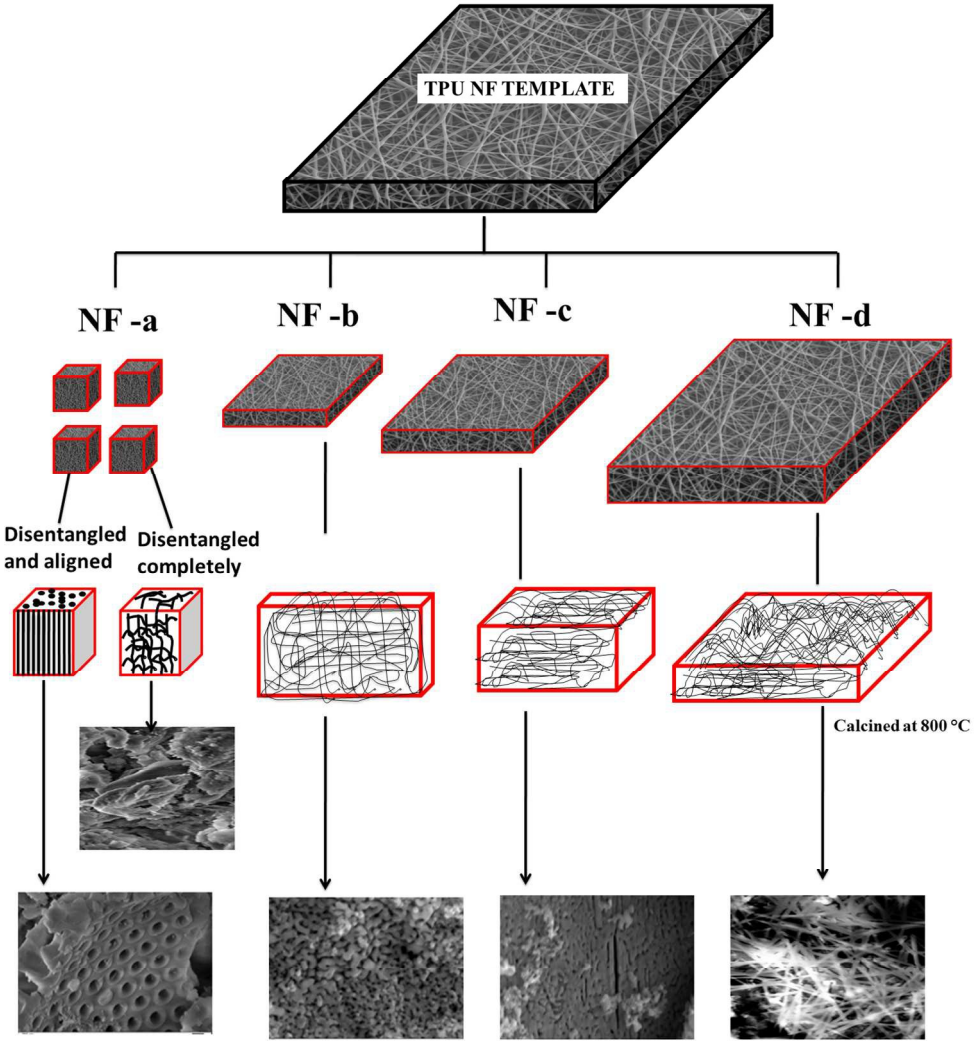

414x449mm (96 x 96 DPI)